Simulation of the Electron Energy Relaxation in a Weakly Ionized Plasma

K. G. Müller * and W. O. Müller

Universität Essen — Gesamthochschule

(Z. Naturforsch. **30 a**, 1553–1559 [1975]; received August 18, 1975)

The motion of electrons in a weakly ionized plasma under the influence of an electric field is simulated by a Monte Carlo method. Elastic and inelastic electron-atom collisions are taken into account using the experimental cross sections. In an application to a low pressure argon positive column the temporal and spatial relaxation of the electron energy distribution is calculated for high electric fields ($30 \leqq E/p_0 \leqq 305$ V/cm Torr). The influence of the wall recombination and the anisotropy due to the high field can be shown.

1. Introduction

The motion of electrons in a weakly ionized plasma under the influence of an electric field $\boldsymbol{E}$ can be described by the electron distribution function $f(\boldsymbol{r}, \boldsymbol{v}, t)$. The usual method to determine f is an analytical or numerical solution of the Boltzmann equation. However, these solutions are limited by a set of approximations, which restrict their applicability. The common basic assumptions are:

- homogeneity $(\partial f/\partial \boldsymbol{r} = 0)$,
- stationarity $(\partial f/\partial t = 0)$,
- weak anisotropy, which allows the expansion

$$f(\boldsymbol{v}) = f^0(v) + f^1(v)\cos\vartheta\,. \tag{1}$$

Here, ϑ is the angle between the velocity $\boldsymbol{v}$ and the direction opposite to the electric field, and $f^0(v)$ and $f^1(v)$ are the first two coefficients of a spherical-harmonics expansion. The applicability of Eq. (1) can be formulated by

$$|f^1(v)/f^0(v)| \ll 1\,. \tag{2}$$

In the following, we use the corresponding ratio

$$A = \int_0^\infty f^1(v)\,\mathrm{d}^3v \Big/ \int_0^\infty f^0(v)\,\mathrm{d}^3v = 3\langle\cos\vartheta\rangle \tag{3}$$

as a measure for the anisotropy.

Time-dependent solutions are either based on the approximation of weak anisotropy (see e.g. Polman [1]) or are limited to a constant collision frequency (Baraff and Buchsbaum [2]). Furthermore, these authors assume an isotropic differential cross section for the collisions between the electrons and the neutrals.

* Reprint requests to Prof. Dr. K. G. Müller, Universität Essen — Gesamthochschule, *D-4300 Essen*, Unionstr. 2.

By a Monte Carlo method, the electron distribution function can be calculated without these approximations. Here, the random walk of test electrons in an external electric field is simulated. Monte Carlo methods have been applied by Englert [3], Sakai, Tagashira and Sakamoto [4], Thomas and Thomas [5] and Makabe, Goto and Mori [6] to calculate energy distribution functions and transport coefficients of electrons in noble gases. The transport coefficients show fair agreement with the numerous experimental data. Due to the lack of experimental data the calculated energy distributions could not be checked satisfactorily. Recently, Lergon and Müller [7] have investigated the spatial relaxation of the electron energy in field direction. They measured a set of space-dependent distribution functions in a low pressure argon discharge at high electric fields.

In this paper we apply the Monte Carlo method to this relaxation experiment. Furthermore, we use a Monte Carlo simulation to investigate the transition from a weak to a high anisotropy with increasing field strength. Thus, the region of the validity of the approximation (1) can be shown. We generate the corresponding energy distributions by a time-dependent relaxation.

We pursue this program in the following way. In Section 2 we develop a model for the motion of electrons, which can be simulated by the method described in Section 3. In Section 4 we apply the Monte Carlo method to relaxation phenomena in argon discharges.

2. Model

We study the motion of single test electrons in a neutral gas under the influence of an electric field. The field is assumed to be parallel to the z-direction

and constant between two succeeding collisions of an electron. To investigate inhomogeneous, nonstationary and anisotropic situations, the motion of an electron is described by the speed v and the angle ϑ as a function of the space coordinate z and the time t.

For the electrons we take into account elastic collisions with the neutrals and inelastic collisions yielding excitation and ionization. A low degree of ionization is assumed, so that Coulomb collisions and volume recombination can be neglected *.

For the collisions the neutrals are assumed to be at rest, which yields a total collision frequency

$$\nu = N q v \tag{4}$$

with

$$q = \sum_k q_k = \sum_k \int \sigma_k \, \mathrm{d}^2\Omega \,, \tag{5}$$

q: total collision cross section,
q_k: total cross section for collisions of the type k,
σ_k: differential cross section for collisions of the type k,
N: density of the neutral gas.

The following energy losses for a test electron are used: for an elastic collision:

$$\Delta\varepsilon = (2\,m/M)\,(1-\cos\chi) \tag{6}$$

for an excitation of an atom from the ground level to the level m:

$$\Delta\varepsilon = \varepsilon_m \tag{7}$$

for an ionization of an atom:

$$\Delta\varepsilon = \varepsilon_\mathrm{i} + (\varepsilon - \varepsilon_\mathrm{i})/2 \tag{8}$$

m, M: mass of electron, atom,
χ: scattering angle,
ε_m: excitation energy,
ε_i: ionization energy,
ε: electron energy before the collision.

Equation (8) means, that the total kinetic energy after an ionizing collision is shared equally by the primary and secondary electron **.

* The degree of ionization (n/N) must be small compared with a critical degree of ionization $(n/N)_\mathrm{crit}$, which can be calculated by equating the electron-electron collision frequency

$$\nu_\mathrm{ee} = \frac{4\sqrt{2\pi}}{3}\, n \left(\frac{e^2}{4\pi\varepsilon_0 k T}\right)^2 \left(\frac{k T}{m}\right)^{\frac{1}{2}} \ln\Lambda$$

(see Shkarofsky [8]) with the corresponding frequency for energy transport, which in our case is given by the frequency for inelastic collisions.

With respect to particle loss we distinguish two cases. In the t-dependent case (case A) we neglect particle losses and study temporal relaxation processes. In the z-dependent case (case B) we take into account particle losses at the wall and study spatial relaxation processes.

To apply case B to the positive column, we introduce the following usual assumptions for the motion of electrons in the positive column:

- The influence of the radial electric field on the energy distribution is negligible.
- The axial electric field is constant along the radius.

The interaction of the electrons with the wall is taken into account by the following model. Adjacent to the wall a sheath exists with a potential barrier Φ_W, which reflects electrons with

$$\tfrac{1}{2}\, m\, v_\perp^2 < e\,|\,\Phi_\mathrm{W}\,| \tag{9}$$

and annihilates electrons with

$$\tfrac{1}{2}\, m\, v_\perp^2 \geqq e\,|\,\Phi_\mathrm{W}\,| \tag{10}$$

by recombination. Here, e is the elementary charge an $v_\perp$ is the velocity perpendicular to the wall. The electron density n is assumed to be radially constant. The potential barrier Φ_W as a function of z can be calculated by the requirement, that in a quasineutral positive column the z-component j_z of the electric current density is independent of z:

$$\partial j_z/\partial z = 0\,. \tag{11}$$

Neglecting the contribution of the ions, we find:

$$j_z = e\,n\langle v_\parallel\rangle \tag{12}$$

where $\langle v_\parallel\rangle$ is the mean electron velocity parallel to the field. A mean velocity, which fulfils Eq. (12), can be guaranteed by a z-dependent wall loss, which is regulated by the potential barrier Φ_W.

3. Simulation Method

3.1. Random walk of a test electron

Since in our model Coulomb interactions are neglected, each electron performs an independent random walk under the influence of an electric field.

** Measurements of the energy distribution of the secondary electrons show a peak at the energy of approximately 4 eV independently of the collision energy in the range of 25–300 eV [9, 10]. As in our calculations the energy ε is about 25 eV, our assumption with respect to the energy of the secondary and the scattered primary electrons is justified.

To construct an electron distribution $f(\boldsymbol{r}, \boldsymbol{v}, t)$, we simulate the random walk of a sample of test electrons by a Monte Carlo method. According to our model, each collision of a test electron is determined by four random variables,

- the time of free flight τ,
- the index k, defining the type of collision,
- the polar scattering angle χ,
- the azimuthal scattering angle ψ.

For each random variable, a probability distribution can be derived. With help of these distributions the variables τ, k, χ, ψ are generated by corresponding random numbers R^τ, R^k, $R_k{}^\chi$, $R_k{}^\psi$. Since the random numbers usually are uniformly distributed between 0 and 1, they have to be transformed to the actual distribution.

Between two succeeding collisions the dynamical state of a test electron changes from (v_0, ϑ_0, z_0) to (v, ϑ, z) with

$$v \sin\vartheta = v_0 \sin\vartheta_0 , \tag{13}$$

$$v \cos\vartheta = v_0 \cos\vartheta_0 + (e\,E/m)\,\tau , \tag{14}$$

$$z = z_0 + v_0 \cos\vartheta_0\,\tau + (e\,E/2\,m)\,\tau^2 . \tag{15}$$

For the time of free flight the probability distribution

$$g(\tau) = \nu(\tau) \exp\left(-\int \nu(\tau')\,\mathrm{d}\tau'\right) \tag{16}$$

holds, so that τ and its corresponding random number R^τ are connected by

$$R^\tau = \exp\left(-\int \nu\,\mathrm{d}\tau'\right) . \tag{17}$$

An inversion of Eq. (17) leads to $\tau(R^\tau)$ (see Appendix).

The type k of collision is determined by the random number R^k with help of

$$\sum_{i=0}^{k-1} q_i/q < R^k \leqq \sum_{i=0}^{k} q_i/q . \tag{18}$$

Similarly the random numbers R^χ and R^ψ define the scattering angles χ and ψ by

$$R_k{}^\chi = \int_0^\chi \mathrm{d}\chi \sin\chi \int_0^{2\pi} \mathrm{d}\psi\, \sigma_k(\varepsilon, \chi, \psi)/q_k , \tag{19}$$

$$R_k{}^\psi = \int_0^\psi \mathrm{d}\psi \int_0^{\pi} \mathrm{d}\chi \sin\chi\, \sigma_k(\varepsilon, \chi, \psi)/q_k . \tag{20}$$

By this operation, the dynamical state of the test electron after the next collision can be calculated. By an iteration of this procedure, a random walk of the test electron can be simulated.

3.2. Electron distribution function

An individual electron l, starting at the time t_0 and the position $\boldsymbol{r}_0$ performs a random walk $(\boldsymbol{r}_l(t), \boldsymbol{v}_l(t))$ in the electric field. For this random walk we can construct a contribution to the energy distribution by averaging

- in the t-dependent case A over the position $\boldsymbol{r}_l(t)$ yielding

$$F(\varepsilon, t) = \frac{1}{L\,\delta} \sum_l 1 ; \quad \varepsilon - \delta/2 < \frac{m}{2} v_l(t)^2 \leqq \varepsilon + \delta/2 \tag{21}$$

  and

- in the z-dependent case B over all times at which a test electron is located at the position z yielding

$$F(\varepsilon, z) = \frac{1}{\delta} \sum_l \frac{1}{v_{\|,l}} \Big/ \sum_{l=1}^{L} \frac{1}{v_{\|,i}} ;$$

$$\varepsilon - \frac{\delta}{2} < \frac{m}{2} v_l{}^2(z) \leqq \varepsilon + \frac{\delta}{2} . \tag{22}$$

By the factor $1/v_{\|,l}$ the contribution of the l-th test electron to the distribution function is weighted with the stay time in the interval $(z, z + \mathrm{d}z)$. L is the number of test electrons and δ is the sampling energy interval. To achieve a sufficient accuracy, we choose in our application $L > 1000$ and $\delta \cong 1$ eV.

As the simulation is based on the same assumptions underlying the Boltzmann equation applied to our model, in the limit $L \to \infty$, $\delta \to 0$ the distribution functions (21 and 22) are solutions of the corresponding Boltzmann equation.

4. Application

In the following we apply our model to the motion of electrons in an argon gas under the influence of an electric field.

4.1. Elementary processes

In our model we distinguish elastic collisions and the inelastic collisions excitation and ionization with the cross sections q_{el}, q_x and q_i and the corresponding energy losses (6), (7) and (8). According to Eq. (5) we split up the total cross section q into its components:

$$q = q_{\mathrm{el}} + q_\mathrm{i} + q_x . \tag{23}$$

Figure 1 shows the experimental cross sections used in our calculations. On the basis of experimental and theoretical data the differential cross section for

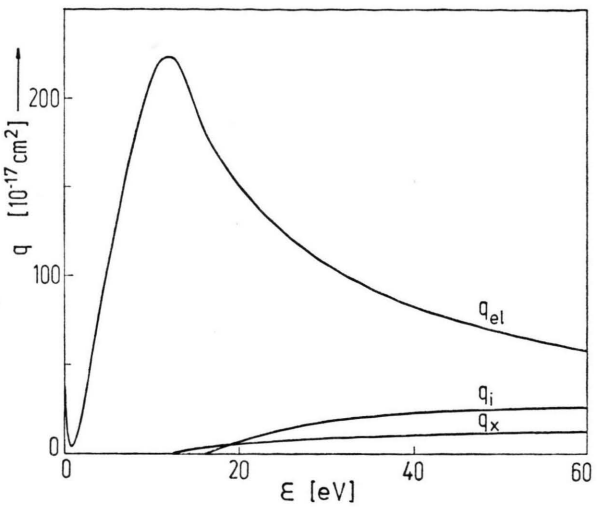

Fig. 1. Cross sections for argon versus electron energy. q_{el}: elastic scattering cross section according to Massey and Burhop [11]; q_x: excitation cross section according to Schaper and Scheibner [12]. In the region $\varepsilon > \varepsilon_i$, the approximation used by Sakai and co-workers [4] is used; q_i: ionization cross section according to Rapp and Englander-Golden [13].

elastic collisions (see Fig. 2) is approximated by

$$\frac{4\pi\cdot\sigma_{el}}{q_{el}} = \begin{cases} \beta[0.75(1-\cos\chi)]^{\beta-1} & \text{for } \cos\chi \geqq -1/3 \\ \beta[1.5(1+\cos\chi)]^{\beta-1} & < -1/3 \end{cases} \tag{24}$$

with

$$\beta = 1/(1+(\varepsilon/10\,\text{eV}))^2 . \tag{25}$$

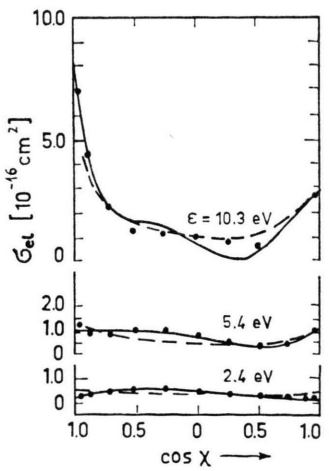

Fig. 2. Elastic differential scattering cross section $\sigma_{el}(\varepsilon, \chi)$ for argon versus scattering angle χ. ····: Ramsauer and Kollath [14] (exp.); ———: Hoeper, Franzen and Gupta [15] (theor.); — — —: analytical approximation according to Equation (24).

The inelastic collisions are assumed isotropic, since measurements of the angular distributions of the inelastically scattered electrons at low energies (20 – 30 eV) show only a small anisotropy in forward direction [16].

4.2. *Time-dependent Simulation (Case A)*

By a Monte Carlo method we study a sample of several thousand test electrons starting with an initial mean energy $\langle\varepsilon\rangle = 5.3$ eV in the electric field (30 V/cm Torr $\leqq E/p_0 \leqq$ 305 V/cm Torr); the initial mean energy corresponds to a reduced electric field of approximately 3 V/cm Torr in the relaxated case. A similar calculation for helium has been performed by Englert. In agreement with his results, we find for argon two stages for the relaxation process, which can be interpreted as follows. In the first stage the electrons are heated up; the mean energy is raised close to its final value; elastic collisions dominate and energy losses can be neglected. In the second stage the energy distribution approaches its final time-independent form due to several inelastic collisions. Since the ionization is not compensated by loss processes, the electron density increases in time. The relaxation times t_R, defined by the duration of the first stage of the relaxation process, are of the order

$$t_R\, p_0 \cong 2\cdot 10^{-7}\,\frac{\text{Vs}}{\text{cm}} \Big/ \frac{E}{p_0} . \tag{26}$$

Figure 3 shows the relaxated energy distributions as a function of the reduced electric field. The distribution for $E/p_0 = 100$ V/cm Torr is practically identical with that one calculated by Golant [17] for $E/p_0 =$ 104 V/cm Torr by means of the approximation (1).

The Monte Carlo method provides the possibility to calculate the anisotropy A of Eq. (3) (see Fig. 4,

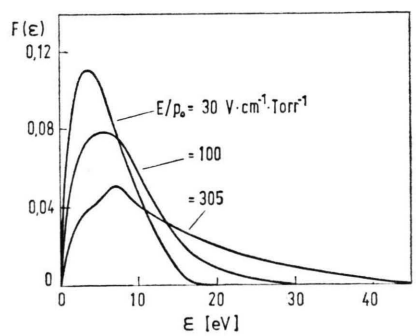

Fig. 3. Calculated electron energy distribution $F(\varepsilon)$ for different values of E/p_0.

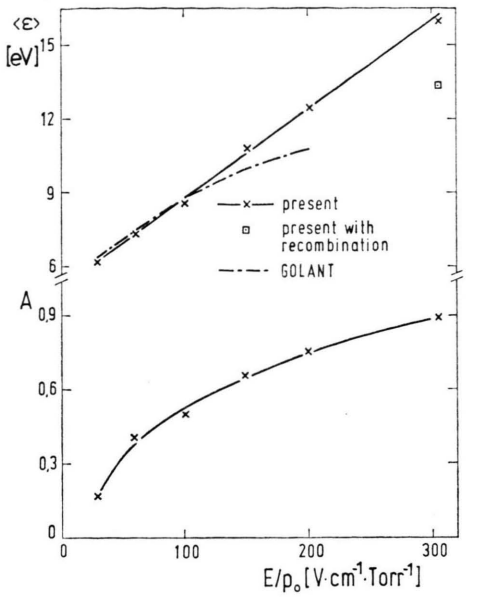

Fig. 4. Mean electron energy $\langle\varepsilon\rangle$ and anisotropy A versus E/p_0.

lower half) and thus to check the assumption of small anisotropy. In Fig. 4, upper half, the calculated mean energy is shown and compared with Golant's solution. For E/p_0 more than 100 V/cm Torr the mean energy of this work increases more than that one of Golant due to the increasing influence of the anisotropy. To demonstrate the influence of the

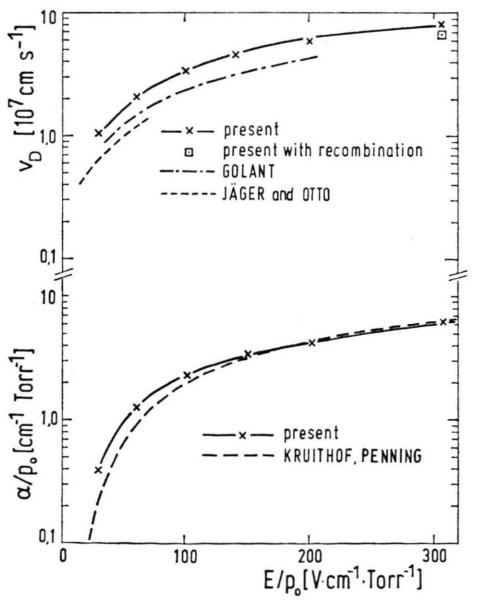

Fig. 5. Drift velocity v_D and first Townsend coefficient α/p_0 versus E/p_0.

recombination we have presented in Fig. 4 the value for $E/p_0 = 305$ V/cm Torr calculated for the case B (Section 4.3).

In Fig. 5, upper half, the calculated drift velocity v_D is compared with the theoretical values of Golant and the experimental ones of Jäger and Otto [18]. The difference between the two theoretical curves is due to the different models with respect to anisotropy, but there still remains a disagreement between theoretical and experimental values, which partially can be explained by the effect of recombination upon the drift velocity. Due to recombination, for $E/p_0 = 305$ V/cm Torr the drift velocity of case B is reduced by 16% compared with that one of case A. The calculated Townsend coefficient, α/p_0, plotted in Fig. 5, lower half, shows good agreement with the experimental values of Kruithof and Penning [19]. Our calculations give a critial degree of ionization between $(n/N)_{\text{crit}} = 3\%$ for $E/p_0 = 305$ V/cm Torr and $(n/N)_{\text{crit}} = 0.02\%$ for $E/p_0 = 30$ V/cm Torr.

4.3. Space-dependent Simulation (Case B)

The Monte Carlo method is applied to simulate the spatial relaxation of an electron energy distribution in a positive column behind a constriction of the tube. This effect has been investigated experimentally by Lergon and Müller [7]. Here we apply case B of Sec. 2 including recombination. With respect to these experimental investigations, we choose parameters as follows:

argon pressure: $p = 3.6 \cdot 10^{-3}$ Torr ;

electric field: $E = \begin{cases} 6.6 \text{ V/cm}, & 0 < z \leqq 0.6 \text{ cm}, \\ 1.2, & 0.6 < z \leqq 15, \\ 1.1, & 15 < z ; \end{cases}$

initial drift velocity: $v_D = 6.8 \cdot 10^7$ cm/s ;

initial mean energy: $\langle\varepsilon\rangle = 13$ eV .

These parameters yield a critical electron density $n_{\text{crit}} = 4 \cdot 10^{12}$ cm^{-3}, which is much larger than the experimentally measured density of about 10^9 cm^{-3}.

Figure 6 shows the resulting relaxated energy distributions in comparison with those of Lergon and Müller. The existence and the shift of the peaks during the relaxation can be explained qualitatively in the following way. A sample of test electrons, representing a peak, drifts in field direction without any appreciable energy loss, until the inelastic collisions come into play. Then the peak is reduced due to excitation and ionization and a new peak is

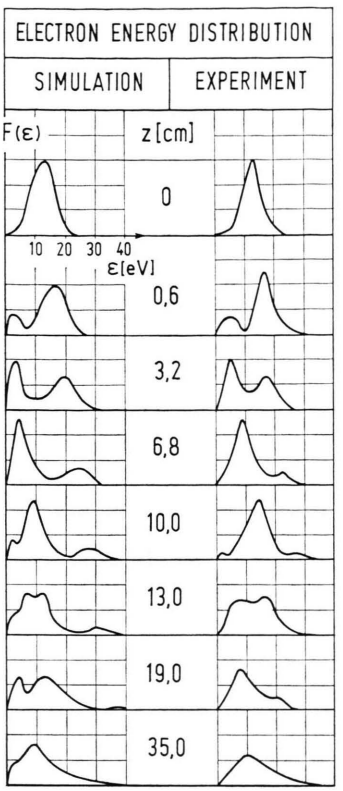

Fig. 6. Spatial relaxation of the electron energy distribution. Right: experiment of Lergon and Müller [7]; left: simulation of present work.

formed by the electrons having suffered an inelastic energy loss. The distance of the two peaks can be interpreted as a mean inelastic energy loss. This relaxation, found experimentally is confirmed by our calculation. However due to the simplified description of the inelastic energy loss, the distance of the peaks differ. At $z = 35$ cm the energy distributions practically are relaxated to the final distribution. Here the main features of the experimental and the simulated curves agree.

In our model the recombination at the wall has been regulated by a suitable choice of the wall potential in accordance with the continuity Equation (12). To satisfy this equation the wall potential has been approximated by $|\Phi_W| = 19.4$ V for $z < 15$ cm and $|\Phi_W| = 24$ V for $z \geqq 15$ cm.

We can compare the relaxated distribution of our calculation with the corresponding distribution of case A (Fig. 3) and find, that the recombination at the wall mainly reduces the tail of the energy distribution. This is due to the high potential barrier Φ_W. The tail of the relaxated distribution calculated with recombination is in agreement with the experiment.

4.4. *Concluding Remarks*

By this application we have demonstrated the importance of the Monte Carlo method for calculating the transport properties of electrons in a range of parameters, which is hardly accessible to the direct solution of the Boltzmann equation. Especially for high anisotropies and for non-stationary or inhomogeneous situations including boundary conditions the Monte Carlo method proofs to be superior.

We thank the 'Ministerium für Wissenschaft und Forschung des Landes Nordrhein-Westfalen' for financial support. Calculations were carried out on the IBM 370/168 computer of the University of Bonn.

Appendix

For the solution of Eq. (17) we regard two cases:

a) For a constant collision frequency ν_0, τ is simply given by

$$\tau = -\frac{1}{\nu_0}\ln(R^\tau)\,. \tag{27}$$

b) For a speed-dependent collision frequency, Eq. (17) can be written in the form

$$-\ln(R^\tau) = \left(\frac{m}{e}\right)\left(\frac{N}{E}\right)\int_{v_0}^{v}\frac{q(v)\,v\,dv}{\cos\vartheta'} \tag{28}$$

where v and ϑ' are related by (13). Assuming that the speed dependence of the total collision cross section can be approximated by a polynomial

$$q(v) = \sum_{m=1}^{5} c_m\, v^m \tag{29}$$

we can integrate in (28) and obtain

$$-\ln(R^\tau) = \left(\frac{m}{e}\right)\left(\frac{N}{E}\right)\Bigg[\cos\vartheta\sum_{m=1}^{7} b_m\, v^m - \cos\vartheta_0\sum_{m=1}^{7} b_m\, v_0{}^m + b_2\, v_\perp^2\ln\left(\frac{v(1+\cos\vartheta)}{v_0(1-\cos\vartheta_0)}\right)\Bigg] \tag{30}$$

with

$$\begin{aligned} b_1 &= 2\,c_1\,v_\perp^2/3 + 8\,c_3\,v_\perp^4/15 + 16\,c_5\,v_\perp^6/35\,,\\ b_2 &= c_0/2 + 3\,c_2\,v_\perp^2/8 + 5\,c_4\,v_\perp^4/16\,,\\ b_3 &= b_1/(2\,v_\perp^2)\,,\\ b_4 &= c_2/4 + 5\,c_4\,v_\perp^2/24\,, \end{aligned} \tag{31}$$

$b_5 = c_3/5 + 6\, c_5\, v_\perp^2/35$,

$b_6 = c_4/6$,

$b_7 = c_5/7$.

Equation (30) has a unique solution for $\cos\vartheta$, which is determined numerically. Knowing $\cos\vartheta$, the change of the dynamical state during the free flight of an electron can be calculated by (13), (14), (15). For our calculations we approximated q by (29) for $\varepsilon \leqq 15$ eV and by $q \sim 1/v$ (constant collision frequency) for $\varepsilon > 15$ eV.

[1] J. Polman, Physica **54**, 305 [1971].
[2] G. A. Baraff and S. J. Buchsbaum, Phys. Rev. **130**, 1007 [1963].
[3] G. W. Englert, Z. Naturforsch. **26 a**, 836 [1971].
[4] Y. Sakai, H. Tagashira, and S. Sakamoto, J. Phys. B, **5**, 1010 [1972].
[5] R. W. L. Thomas and W. R. L. Thomas, J. Phys. B, **2**, 562 [1969].
[6] T. Makabe, T. Goto, and T. Mori, 2nd Int. Conf. Gas Discharges, IEEE, London 1972, p. 379.
[7] H. G. Lergon and K. G. Müller, Z. Phys. **268**, 157 [1974].
[8] I. P. Shkarofsky, T. W. Johnston, and M. P. Bachynski, The Particle Kinetics of Plasma, Addison-Wesley Publ. Co., Dordrecht 1966, p. 334.
[9] H. Massey and C. Mohr, Proc. Roy. Soc. A **140**, 613 [1933].
[10] H. Ehrhardt, K.-H. Hesselbacher, and K. Willmann, Z. Naturforsch. **22 a**, 444 [1967].
[11] H. Massey and E. Burhop, Electronic and Ionic Impact Phenomena, Vol. I, Oxford University Press, Oxford 1969, p. 404.
[12] M. Schaper and H. Scheibner, Beitr. Pl. Physik **9**, 54 [1969].
[13] D. Rapp and P. Englander-Golden, J. Chem. Phys. **42**, 1464 [1965].
[14] C. Ramsauer and R. Kollath, Ann. Phys. **5**, 529 [1932].
[15] S. Hoeper, W. Franzen, and R. Gupta, Phys. Rev. **168**, 50 [1968].
[16] H. Massey and E. Burhop, Electronic and Ionic Impact Phenomena, Vol. I, Oxford University Press, Oxford 1969, p. 343.
[17] V. E. Golant, Sov. Phys. Tech. Phys. **4**, 680 [1959].
[18] G. Jäger and W. Otto, Z. Physik **169**, 517 [1962].
[19] A. A. Kruithof and F. M. Penning, Physica **3**, 515 [1936].